Mechanism of Peroxynitrite Oxidation of Aliphatic CH Bonds in Saturated and Unsaturated Hydrocarbons. A Theoretical Model for the CH Oxidation of Lipids

Gennady V. Shustov, Richard Spinney, and Arvi Rauk*

Contribution from the Department of Chemistry, The University of Calgary, Calgary, Alberta, Canada T2N 1N4

Received September 30, 1999. Revised Manuscript Received December 2, 1999

Abstract: The oxidation of aliphatic CH bonds in methane, propane, isobutane, propene, and 1,4-pentadiene with peroxynitrous acid and peroxynitrite anion has been studied computationally with the B3LYP, MP2, and QCISD(T) levels of theory. The CCD, CISD, and CCSD(T) methods were also used for the parent systems, methane−ONOOH and methane−$ONOO^-$. Three pathways were considered: path a, direct oxygen insertion into a C−H bond (two-electron oxidation); path b, H atom abstraction leading to alkyl radicals (one-electron oxidation); and path c, O−O bond homolysis of ONOOH (initial oxidation by hydroxyl radicals). Transition structures were located for path a which correspond to a concerted electrophilic oxygen insertion into the CH leading to the corresponding alcohols. At the QCISD(T)/6-31+G*//B3LYP/6-31+G* level, the activation barriers for the path a oxidation of methane, propane, isobutane, propene, and 1,4-pentadiene with ONOOH are 30.8, 18.1, 17.0, 21.1, and 17.8 kcal mol^{-1} and with $ONOO^-$ they are 35.8, 29.4, 26.3, 25.0, and 14.0 kcal mol^{-1}, respectively. The direct abstraction of the hydrogen atom from the hydrocarbons by these oxidants (path b) yielding alkyl radicals is thermodynamically much less favorable than the two-electron oxidation even for 1,4-pentadiene (model for lipids). The calculated lower limit for the free energy of activation for the two-electron CH oxidation of 1,4-pentadiene with ONOOH ($\Delta G^{\neq}_{298}$ = 20.5 kcal mol^{-1}) is higher than the free energy of homolysis of the O−O bond (path c) in ONOOH (ΔG_{298} = 12.2−17.4 kcal mol^{-1}, theoretical and experimental estimates). This supports the hypothesis that the reactive species in hydrocarbon oxidations by peroxynitrous acid, and in lipid peroxidation induced by peroxynitrous acid in the presence of air, is the discrete hydroxyl radical formed in the homolysis of this acid.

Introduction

Peroxynitrite oxidation of organic substrates is a very important biochemical process[1,2,3] and, at the same time, can be considered as a potentially useful method for synthetic organic chemistry. It has been believed[1,2] that the active oxidant in this process in the absence of CO_2 is the unstable peroxynitrous acid, ONOOH (pK_a = 6.5−6.8),[4] which is generated from the relatively stable peroxynitrite anion, $ONOO^-$, at physiological pH or lower. In vivo, the latter is formed in the reaction of nitric oxide with superoxide.[4,5] In synthetic practice, salts of peroxynitrous acid can be prepared by various methods including ozonation of azides,[6a] oxidation of nitrous acid with hydrogen peroxide,[6b] and the reaction of nitric oxide with tetramethylammonium superoxide.[6c]

Peroxynitrous acid can oxidize organic substrates, e.g. RH, either directly (Scheme 1, paths a and/or b) or through homolysis to the more reactive hydroxyl radical (Scheme 1, path c). Either molecule-induced homolysis (path b) or unimolecular homolysis (path c) may be responsible for the apparent involvement of free radicals in peroxynitrite oxidations. Even in recent studies,[7−9] the participation of the discrete hydroxyl radical in peroxynitrite oxidations has been called in question. The complex kinetic behavior in water has even led to the postulate of a reactive "hydroxyl radical-like" intermediate.[1,10−12] Current understanding[13] of the pH dependent aqueous behavior of this oxidant does

Scheme 1

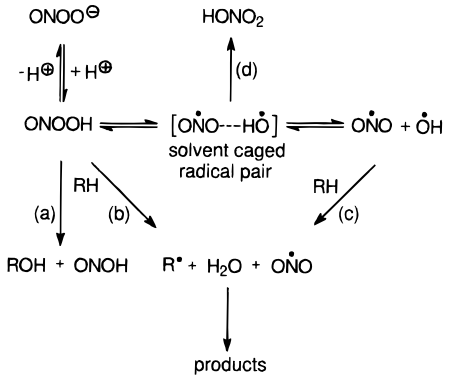

(1) Pryor, W. A.; Squadrito, G. L. *Am. J. Physiol. (Lung Cell. Mol. Physiol. 12)* **1995**, *268*, L699.

(2) Beckman, J. S. In *Nitric Oxide. Principles and Actions*; Lancaster, J. Jr., Ed.; Academic Press: San Diego, 1996; pp 1−82.

(3) (a) Muijsers, R. B. R.; Folkerts, G.; Henricks, P. A. J.; Sadeghi-Hashjin, G.; Nijkamp, F. P. *Life Sci.* **1997**, *60*, 1833. (b) Fukuto, J. M.; Ignarro, L. J. *Acc. Chem. Res.* **1997**, *30*, 149. (c) Balavoine, G. G. A.; Geletii, Yu. V. *Nitric Oxide: Biol. Chem.* **1999**, *3*, 40.

(4) Kissner, R.; Nauser, T.; Bugnon, P.; Lye, P. G.; Koppenol, W. H. *Chem. Res. Toxicol*. **1997**, *10*, 1285.

(5) Huie, R. E.; Padmaja, S. *Free Radical Res.* **1993**, *18*, 195.

(6) (a) Uppu, R. M.; Squadrito, G. L.; Cueto, R.; Pryor W. A. *Methods Enzymol.* **1996**, *269*, 285, 311. (b) Uppu, R. M.; Pryor, W. A. *Methods Enzymol.* **1996**, *269*, 322. (c) Bohle, D. S.; Glassbrenner, P. A.; Hansert, B. *Methods Enzymol.* **1996**, *269*, 302.

(7) Goldstein, S.; Squadrito, G. L.; Pryor, W. A.; Czapski, G. *Free Radical Biol. Med.* **1996**, *21*, 965.

(8) Richeson, C. E.; Mulder, P.; Bowry, V. W.; Ingold, K. U. *J. Am. Chem. Soc.* **1998**, *120*, 7211.

(9) Koppenol, W. H.; Kissner, R. *Chem. Res. Toxicol.* **1998**, *11*, 87.

10.1021/ja993533k CCC: $19.00
Published on Web 01/29/2000

Scheme 2

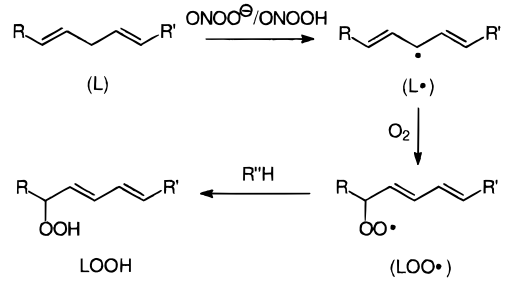

not require the introduction of such a species except as a cage within which competitive rearrangement[11] to nitrate can take place (Scheme 1, path d).

Operation of pathways c and d requires homolysis of the O−O bond in ONOOH. Experimental estimates[8,14] of the bond dissociation enthalpy for the O−O bond in aqueous solution vary from 18 to 23.2 kcal mol^{-1}, with theoretical gas phase estimates from 20.3 (CBS-Q)[11] to 22.0 kcal mol^{-1}(G2).[15] The half-life of ONOOH in water is about 1 s.[13] Activation barriers for H abstraction from alkanes by hydroxyl radical are in the range 2−4 kcal mol^{-1} (7.4 kcal mol^{-1} for CH_4).[16]

Among biomolecules, lipids containing polyunsaturated fatty acids are key targets of peroxynitrite oxidation.[17,18] The well-known cytotoxic properties of ONOO$^-$/ONOOH are to a considerable extent caused by the ability of this reagent to damage cell membranes. It was found[17,18] that lipid peroxidation is the main channel of the interaction of lipids with ONOOH in the presence of O_2. This implies that there is a mechanism whereby ONOOH induces formation of lipid free radicals. The radicals (L•) are intercepted by dioxygen and yield hydroperoxides (LOOH) (Scheme 2).[18a] Hydroxyl and nitrogen containing products were also identified in the reaction mixtures along with the lipid hydroperoxides.[18a]

One can suppose that the formation of the lipid free radicals is triggered by the hydroxyl radical generated from ONOOH (Scheme 1, path c). However, the possibility that peroxynitrous acid itself is able to abstract a hydrogen atom from a methylene group of a lipid (Scheme 1, path b) needs to be considered.

Scheme 3

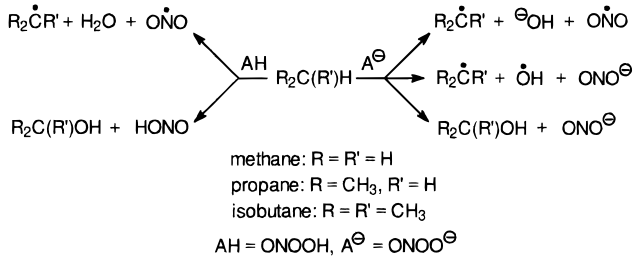

Scheme 4

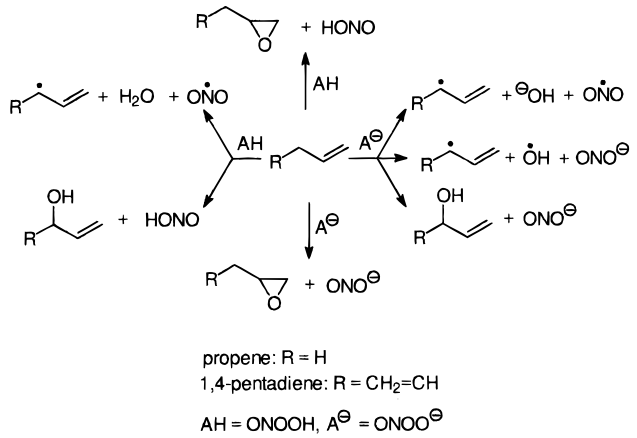

There is yet only one published[19] work on the oxidation of saturated hydrocarbons with peroxynitrous acid. Rudakov et al.[19] have shown that alcohols and the corresponding ketones are major products of the reaction under strictly anaerobic conditions. From relative rate constants and kinetic isotope effects, the authors concluded that the reactive species is peroxynitrous acid itself (or a decomposition product, the ONOO• radical) but not HO•.

Recently, Houk et al.[10,20] and Bach et al.[21] have theoretically studied some oxidative reactions of ONOOH and ONOO$^-$. In particularly, these groups investigated transition states for epoxidation of ethylene[10,20,21] and propene,[21] and for oxidation of the heteroatoms in ammonia,[10] trimethylamine,[21] hydrogen sulfide,[10] dimethyl sulfide,[21] and trimethylphosphine.[21]

Here we report the first theoretical study of the mechanism of the oxidation of CH bonds in saturated (methane, propane, and isobutane) and unsaturated hydrocarbons (propene and 1,4-pentadiene) with peroxynitrous acid (Schemes 3 and 4). 1,4-Pentadiene is a close model for lipids, possessing the vulnerable bis-allylic RCH═CHCH$_2$CH═CHR′ fragment.The main purposes of the present work are (a) determination of the nature and energies of the transition states for direct O insertion, (b) estimation of the ability of peroxynitrous acid to induce formation of alkyl free radicals, and (c) comparison of the activation energies of the CH oxidation with the energy of homolysis of the O−O bond in ONOOH as a competitive reaction.

The possibility of the CH oxidation of these hydrocarbons with peroxynitrite anion (Schemes 3 and 4) was also compu-

(10) Houk, K. N.; Condorski, K. R.; Pryor, W. A. *J. Am. Chem. Soc.* **1996**, *118*, 13002.

(11) Bartberger, M. D.; Olson, L. P.; Houk, K. N. *Chem. Res. Toxicol.* **1998**, *11*, 710.

(12) Squadrito, G. L.; Pryor, W. A. *Chem. Res. Toxicol.* **1998**, *11*, 718.

(13) (a) Merenyi, G.; Lind, J. *Chem. Res. Toxicol.* **1997**, *10*, 1216. (b) Merenyi, G.; Lind, J.; Goldstein, S.; Czapski, G. *Chem. Res. Toxicol.* **1998**, *11*, 712. (c) Lymar, S. V.; Hurst, J. K. *Chem. Res. Toxicol.* **1998**, *11*, 714. (d) Coddington, J. W.; Hurst, J. K.; Lymar, S. V. *J. Am. Chem. Soc.* **1999**, *121*, 2438. (e) Merenyi, G.; Lind, J.; Goldstein, S.; Czapski, G. *J. Phys. Chem.* **1999**, *103*, 5685.

(14) Tsai, H.-H.; Hamilton, T. P.; Tsai, J.-H.; van der Woerd, M.; Harrison, J. G.; Jablonsky, M. J.; Beckman, J. S.; Koppenol, W. H. *J. Phys. Chem.* **1996**, *100*, 15087.

(15) (a) Sumathi, R.; Peyerimhoff, S. D. *J. Chem. Phys.* **1997**, *107*, 1872. (b) Bach, R. D.; Ayala, P. Y.; Schlegel, H. B. *J. Am. Chem. Soc.* **1996**, *118*, 12758.

(16) (a)Hu, W.-P.; Rossi, I.; Corchado, J. C.; Truhlar, D. G. *J. Phys. Chem. A* **1997**, *101*, 6911. (b) Melissas, V. S.; Truhlar, D. G. *J. Chem. Phys.* **1993**, *99*, 1013.

(17) (a) Darley-Usmar, V. M.; Mason, R. P.; Chamulirat, W.; Hogg, N.; Kalyanaraman, B. In *Immunopharmacology of Free Radical Species*; Blake, D., Winyard, P. G., Eds.; Academic Press: San Diego, 1995; pp 23−37. (b) Radi, R.; Beckman, J. S.; Bush, K. M.; Freeman, B. A. *Arch. Biochem. Biophys.* **1991**, *288*, 481.

(18) (a) Rubbo, H.; Radi, R.; Trujillo, M.; Telleri, R.; Kalyanaraman, B.; Barnes, S.; Kirk, M.; Freeman, B. A. *J. Biol. Chem.* **1994**, *269*, 26066. (b) Cristol, J. P.; Maggi, M. F.; Guerin, M. C.; Torreilles, J.; Descomps, B. *C. R. Seances Soc. Biol. Fil.* **1995**, *189*, 797. (c) Lamarque, D.; Whittle, B. J. R. *Eur. J. Pharm.* **1996**, *313*, R5. (d) Gadelha, F. R.; Thomson, L.; Fagian, M. M.; Costa, A. D. T.; Radi, R.; Vercesi, A. E. *Arch. Biochem. Biophys.* **1997**, *345*, 243. (e) Keller, J. N.; Kindy, M. S.; Holtsberg, F. W.; St Clair, D. K.; Yen, H.-C.; Germeyer, A.; Steiner, S. M.; Bruce-Keller, A. J.; Hutchins, J. B.; Mattson, M. P. *J. Neurosci.* **1998**, *18*, 687.

(19) Rudakov, E. S.; Lobachev, V. L.; Geletii, Yu. V.; Balavoine, G. G. A. *Russ. J. Org. Chem.* **1996**, *32*, 500.

(20) Houk, K. N.; Liu, J.; DeMello, N. C.; Condorski, K. R. *J. Am. Chem. Soc.* **1997**, *119*, 10147.

(21) Bach, R. D.; Glukhovtsev, M. N.; Canepa, C. *J. Am. Chem. Soc.* **1998**, *120*, 775.

Table 1. Relative Energies[a](kcal mol^{-1}) of the Reactants, Products, and Transition States for the Parent Systems Methane−Peroxynitrous Acid and Methane−Peroxynitrite Anion

species	B3LYP/A[b]	B3LYP/B[b]	B3LYP/C[b]	MP2/A[b]	QCISD(T)/A//B3LYP/A[b]	QCISD(T)/A//MP2/A[b]	QCISD(T)/A//CISD/A[b]	CCSD(T)/A//CCD/A[b]
$CH_4 + ONOOH$	0.0	0.0	0.0	0.0	0.0	0.0	0.0	0.0
TS1	34.5	28.9	31.2	39.9	30.8	41.6	43.7	43.7
$CH_3OH + ONOH$	−40.6	−44.8	−44.0	−46.4	−42.7	−42.5	−43.4	−42.8
$CH_3^{\bullet} + H_2O + ONO^{\bullet}$	5.7	−1.2	0.2	−2.8	5.7	6.8	4.9	8.2
$CH_4 + ONOO^-$	0.0	0.0	0.0	0.0	0.0	0.0	0.0	0.0
TS1A	32.2	27.0	28.4	37.6	35.2	35.9	38.6	35.5
$CH_3OH + ONO^-$	−47.1	−51.2	−51.3	−57.2	−49.2	−49.7	−50.7	−50.8
$CH_3^{\bullet} + OH^- + ONO^{\bullet}$	53.2	46.1	45.6	48.2	53.1	52.8	51.8	54.1
$CH_3^{\bullet} + OH^{\bullet} + ONO^-$	38.4	33.4	34.7	32.6	34.1	33.6	31.7	32.1

[a] Including 0.98 × ΔZPVE for the B3LYP, CISD, and CCD calculations and 0.967 × ΔZPVE for the MP2 calculations. [b] Basis set "A" is 6-31+G(d), "B" is 6-311+G(d,p), and "C" is 6-311++G(3df,2pd).

Table 2. Relative Energies[a](kcal mol^{-1}) of the Reactants, Products, and Transition States for the Systems Propane−Peroxynitrous Acid and Propane−Proxynitrite Anion Derived with the 6-31+G* Basis Set

species	B3LYP	MP2	QCISD(T)//B3LYP	QCISD(T)//MP2	SCIPCM-B3LYP
$(CH_3)_2CH_2 + ONOOH$	0.0	0.0	0.0	0.0	0.0
TS2	18.9	35.3	18.1	39.4	13.9
$(CH_3)_2CHOH + ONOH$	−49.4	−57.0	−53.2	−53.0	−53.6
$(CH_3)_2CH^{\bullet} + H_2O + ONO^{\bullet}$	−2.8	−9.1	−0.3	−1.2	−4.1
$(CH_3)_2CH_2 + ONOO^-$	0.0	0.0	0.0	0.0	0.0
TS2A	27.8	28.9	29.4	30.1	33.9
$(CH_3)_2CHOH + ONO^-$	−56.5	−70.7	−60.2	−60.3	−61.9
$(CH_3)_2CH^{\bullet} + OH^- + ONO^{\bullet}$	44.7	31.6	47.1	47.1	31.2
$(CH_3)_2CH^{\bullet} + OH^{\bullet} + ONO^-$	29.3	23.4	27.5	27.8	23.1

[a] Including 0.98 × ΔZPVE and 0.967 × ΔZPVE for the B3LYP and MP2 calculations, respectively.

tationally studied in the present paper. Certainly, the reactivity of $ONOO^-$ is expected to be considerably lower in the aqueous medium than in the gas phase due to strong hydration of the anion. However, there is a possibility of transfer of the nonsolvated ("naked") peroxynitrite anion into a hydrocarbon medium or inside a cell membrane by a lipophilic counterion like a tetraalkylammonium cation, where it may compete with its neutral conjugate acid. Synthesis of such a reagent, tetramethylammonium peroxynitrite, has been described.[6c]

For completeness of the picture in the case of propene and 1,4-pentadiene, we estimated the activation barriers for a competitive reaction, the epoxidation of C=C bonds with peroxynitrous acid and its anion.

Computational Methods

All ab initio calculations presented here were performed with the Gaussian 94[22a] and Gaussian 98[22b] systems of programs. The geometry optimizations and frequency calculations were carried out at various levels of theory including the B3LYP, MP2, CISD, and CCD methods with the internal 6-31+G*, 6-311+G**, and 6-311++G(3df,2pd) basis sets, using procedures implemented in the Gaussian molecular orbital packages. The energies were refined by single-point calculations at the QCISD(T), CCSD(T), and G2(MP2−B3LYP) levels of theory. The last is a variation of G2(MP2)[23] in which B3LYP geometries and zero-point vibrational energies (ZPVE) are used instead of MP2 geometries and HF ZPVEs. The methods and basis sets used for the calculations of each specific reaction system are shown in Tables1−6. Harmonic frequency analysis verified the nature of the stationary points as minima (all real frequencies) or as transition structures (one imaginary frequency) and was used to provide an estimate of the ZPVE. Zero-point corrections (ΔZPVE) were scaled by 0.98 for the B3LYP, CISD, and CCD levels and by 0.967 for the MP2 level.[24] In the cases of the MP2, CISD, CCD, QCISD(T), and CCSD(T) calculations, the frozen core approximation was used. Total energies and ZPVEs of all species are given in Tables S-1−S-4 of the Supporting Information.

The intrinsic reaction coordinate (IRC)[25] path was traced to check the B3LYP/6-31+G(d) energy profiles for all CH oxidations. Analysis

Table 3. Relative Energies[a] (kcal mol^{-1}) of the Reactants, Products, and Transition States for the Systems Isobutane−Peroxynitrous Acid and Isobutane−Peroxynitrite Anion Derived with the 6-31+G* Basis Set

species	B3LYP	QCISD(T)//B3LYP	SCIPCM-B3LYP
$(CH_3)_3CH + ONOOH$	0.0	0.0	0.0
TS3	15.8	17.0	13.4
$(CH_3)_3COH + ONOH$	−51.6	−56.6	−54.5
$(CH_3)_3C^{\bullet} + H_2O + ONO^{\bullet}$	−5.6	−2.1	−9.0
$(CH_3)_3CH + ONOO^-$	0.0	0.0	0.0
TS3A	25.9	26.3	34.2
$(CH_3)_3COH + ONO^-$	−58.0	−63.0	−62.2
$(CH_3)_3C^{\bullet} + OH^- + ONO^{\bullet}$	41.8	45.4	29.9
$(CH_3)_3C^{\bullet} + OH^{\bullet} + ONO^-$	27.1	26.4	21.8

[a] Including 0.98 × ΔZPVE.

(22) (a) Frisch, M. J.; Trucks, G. W.; Schlegel, H. B.; Gill, P. M. W.; Johnson, B. G.; Robb, M. A.; Cheeseman, J. R.; Keith, T.; Petersson, G. A.; Montgomery, J. A.; Raghavachary, K.; Al-Laham, M. A.; Zakrewski, U. G.; Ortiz, J. V.; Foresman, J. B.; Cioslowski, J.; Stefanov, B. B.; Nanayakkara, A.; Challacombe, M.; Peng, C. Y.; Ayala, P. Y.; Chen, W.; Wong, M. W.; Anders, J. L.; Replogle, E. S.; Gomperts, R.; Martin, R. L.; Fox, D. J.; Binkley, J. S.; Defrees, D. J.; Baker, J.; Stewart, J. P.; Head-Gordon, M.; Gonzalez, C.; Pople, J. A. *Gaussian 94, Revisions D.2 and E.2*; Gaussian, Inc.: Pittsburgh, PA, 1995. (b) Frisch, M. J.; Trucks, G. W.; Schlegel, H. B.; Scuseria, G. E.; Robb, M. A.; Cheeseman, J. R.; Zakrzewski, V. G.; Montgomery, J. A., Jr.; Stratmann, R. E.; Burant, J. C.; Dapprich, S.; Millam, J. M.; Daniels, A. D.; Kudin, K. N.; Strain, M. C.; Farkas, O.; Tomasi, J.; Barone, V.; Cossi, M.; Cammi, R.; Mennucci, B.; Pomelli, C.; Adamo, C.; Clifford, S.; Ochterski, J.; Petersson, G. A.; Ayala, P. Y.; Cui, Q.; Morokuma, K.; Malick, D. K.; Rabuck, A. D.; Raghavachari, K.; Foresman, J. B.; Cioslowski, J.; Ortiz, J. V.; Stefanov, B. B.; Liu, G.; Liashenko, A.; Piskorz, P.; Komaromi, I.; Gomperts, R.; Martin, R. L.; Fox, D. J.; Keith, T.; Al-Laham, M. A.; Peng, C. Y.; Nanayakkara, A.; Gonzalez, C.; Challacombe, M.; Gill, P. M. W.; Johnson, B.; Chen, W.; Wong, M. W.; Andres, J. L.; Gonzalez, C.; Head-Gordon, M.; Replogle, E. S.; Pople, J. A. *Gaussian 98, Revisions A.3*; Gaussian, Inc.: Pittsburgh, PA, 1998.

(23) Curtiss, L. A.; Raghavachari, K.; Pople, J. A. *J. Chem. Phys*. **1993**, *98*, 1293.

(24) Scott, A. P.; Radom, L. *J. Phys. Chem*. **1996**, *100*, 16502.

(25) (a) Gonzalez, C.; Schlegel, H. B. *J. Phys. Chem*. **1990**, *94*, 5523. (b) Gonzalez, C.; Schlegel, H. B. *J. Phys. Chem.* **1991**, *95*, 5853.

Table 4. Energy[a,b] (in kcal mol^{-1}) of Homolysis of Peroxynitrous Acid

level	E_{rel}
B3LYP/6-31+G*	14.1
B3LYP/6-311+G**	10.0
B3LYP/6-311++G(3df,2pd)	13.3
MP2/6-31+G*	10.4
QCISD(T)/6-31+G*//B3LYP/6-31+G*	14.1
QCISD(T)/6-31+G*//MP2/6-31+G*	15.6
QCISD(T)/6-31+G*//CISD/6-31+G*	13.4
CCSD(T)/6-31+G*//CCD/6-31+G*	14.1
SCIPCM-B3LYP/6-31+G*	12.0
G2(MP2−B3LYP)[c]	21.5[d]
expt	18−23[e]

[a] Calculated as the difference between the energy of ONOOH and sum of the energies of a radical pair of OH$^{\bullet}$ and ONO$^{\bullet}$. [b] Including 0.98 × ΔZPVE for the B3LYP, CISD, and CCD calculations and 0.967 × ΔZPVE for the MP2 calculations. [c] G2(MP2-B3LYP) is the same as G2(MP2) (see ref 15b) except that B3LYP/6-31+G* geometries and ΔZPVEs are used. [d] The large difference between the "G2(MP2)" value and the others originates in the difference in treatment of correlation between the 6-311+G(3df,2p) and 6-311G** basis sets (5 kcal mol^{-1}) and the HLC terms (3 kcal mol^{-1}). [e] References 8 and 14.

Table 5. Relative Energies[a] (kcal mol^{-1}) of the Reactants, Products, and Transition States for the Systems Propene−Peroxynitrous Acid and Propene−Peroxynitrite Anion Derived with the 6-31+G* Basis Set

species	B3LYP	QCISD(T)// B3LYP	SCIPCM-B3LYP
CH_2=$CHCH_3$ + ONOOH	0.0	0.0	0.0
TS4	17.9	21.1	17.2
CH_2=$CHCH_2OH$ + ONOH	−44.1	−46.9	−48.5
CH_2=$CHCH_2^{\bullet}$ + H_2O + ONO$^{\bullet}$	−13.4	−10.0	−17.6
CH_2=$CHCH_3$ + $ONOO^-$	0.0	0.0	0.0
TS4A	20.2	25.0	34.0
CH_2=$CHCH_2OH$ + ONO^-	−50.6	−53.3	−56.2
CH_2=$CHCH_2$ + HO^- + ONO$^{\bullet}$	34.1	37.4	21.2
CH_2=$CHCH_2$ + HO$^{\bullet}$ + ONO^-	19.3	18.4	13.0

[a] Including 0.98 × ΔZPVE.

Table 6. Relative Energies[a] (kcal mol^{-1}) of the Reactants, Products, and Transition States for the Systems 1,4-Pentadiene−Peroxynitrous Acid and 1,4-Pentadiene−Peroxynitrite Anion Derived with the 6-31+G* Basis Set

species	B3LYP	QCISD(T)// B3LYP	SCIPCM-B3LYP
$(CH_2$=$CH)_2CH_2$ + ONOOH	0.0	0.0	0.0
TS5	13.2	17.8	11.7
$(CH_2$=$CH)_2CHOH$ + ONOH	−46.2	−49.6	−50.8
$(CH_2$=$CH)_2CH^{\bullet}$ + H_2O + ONO$^{\bullet}$	−27.7	−20.5	−32.0
$(CH_2$=$CH)_2CH_2$ + $ONOO^-$	0.0	0.0	0.0
TS5A	8.4	14.0	27.3
$(CH_2$=$CH)_2CHOH$ + ONO^-	−52.6	−56.0	−59.6
$(CH_2$=$CH)_2CH^{\bullet}$ + HO^- + ONO$^{\bullet}$	19.7	26.9	5.7
$(CH_2$=$CH)_2CH^{\bullet}$ + HO$^{\bullet}$ + ONO^-	5.0	7.9	−2.5

[a] Including 0.98 × ΔZPVE.

of the electronic properties of the B3LYP and MP2 transition structures was performed via natural bond orbital (NBO) analysis.[26] Both singlet and triplet stabilities of the RHF and RB3LYP solutions for these structures have been checked.[27]

The effects of dielectric medium were simulated by single-point SCRF calculations with the SCIPCM model[28] as implemented in Gaussian 94. Heat capacities and entropy corrections were made using scaled (0.98) B3LYP/6-31+G* frequencies and standard statistical procedures within the rigid rotator−harmonic oscillator model[29] to determine enthalpies and free energies at 298 K, 1 atm. Free energies (ΔG_{298}) given below were estimated at standard state = 1 M using ΔS_{298}(1 M). The entropies are related by ΔS(1 M) = ΔS(1 atm) − $\Delta nR \ln(R'T)$, for a unit change in molarity, $\Delta n = 0$ for the homolysis of ONOOH and −1 for the oxidations with ONOOH, and $R = 1.9872$ cal mol^{-1} K^{-1}, $R' = 0.08206$ dm^3 atm M^{-1} K^{-1}, and $T = 298$ K.

Throughout the text, bond lengths are in angstroms and bond angles in degrees.

Chart 1

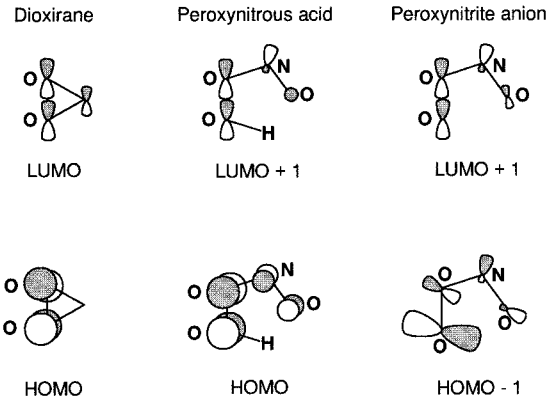

Results and Discussion

Peroxynitrous Acid. Oxidation of CH Bonds in the Saturated Hydrocarbons: (i) Path a. The theoretical picture for the oxidation of CH bonds in methane and propane with *cis*,*cis*-peroxynitrous acid proved to be similar in many respects to that for the dioxirane oxidation[30,31] of these hydrocarbons. The reason is the similarity of the frontier orbitals of both oxidants, which participate in the formation of the transition states of the CH oxidations. Certainly, the oxidative (i.e., electron acceptor) properties of peroxynitrous acid and dioxirane are determined primarily by the low-lying antibonding σ^* orbital of the O−O bond, which is the LUMO for dioxirane and LUMO + 1 for ONOOH (Chart 1; the LUMO of ONOOH is the π^* orbital of the N=O bond). However, the HOMO that constitutes the π^*-like out-of-phase combination of the oxygen nonbonding orbitals, oriented perpendicularly to the molecular plane, may play a certain role as well.

As in the case of the dioxirane oxidation,[30] the MP2 and B3LYP methods predict radically different transition structures and by inference, different reaction mechanisms. The MP2 method exaggerates involvement of the HOMO (π_{OO}^*) of peroxynitrous acid in the formation of the transition states of the oxidation of methane (**TS1**) and propane (**TS2**) (Figure 1). Indeed, in the MP2/6-31+G* structures, **TS1(MP2)** and **TS2-(MP2)**, NBO population analysis shows a net negative charge on the R_2CH hydrocarbon fragment, −0.200e in **TS1(MP2)** and −0.251e in **TS2(MP2)**. The appearance of these charges is a consequence of substantial *proton-transfer character* of the MP2 transition structures caused by the HOMO of peroxynitrous acid, as is evident in the considerable out-of-plane angles, α, 70.4

(26) Glendening, E. D.; Reed, A. E.; Carpenter, J. E.; Weinhold, F. *NBO Version 3.1*.

(27) (a) Schlegel, H. B.; McDouall, J. J. W. In *Computational Advances in Organic Chemistry: Molecular Structure and Reactivity*; Ögretir, C., Csizmadia, I. G., Eds.; Kluwer: Dordrecht, 1991; p 167. (b) Chen, W.; Schlegel, H. B. *J. Chem. Phys.* **1994**, *101*, 5957.

(28) Foresman, J. B.; Keith, T. A.; Wiberg, K. B.; Snoonian, J.; Frisch, M. J. *J. Phys. Chem.* **1996**, *100*, 16098.

(29) McQuarrie, D. A. *Statistical Thermodynamics*; Harper & Row: New York, 1973.

(30) Shustov, G. V.; Rauk, A. *J. Org. Chem.* **1998**, *63*, 5413.

(31) (a) Du, X.; Houk, K. N. *J. Org. Chem.* **1998**, *63*, 6480. (b) Glukhovtsev, M. N.; Canepa, C.; Bach, R. D. *J. Am. Chem. Soc.* **1998**, *120*, 10528.

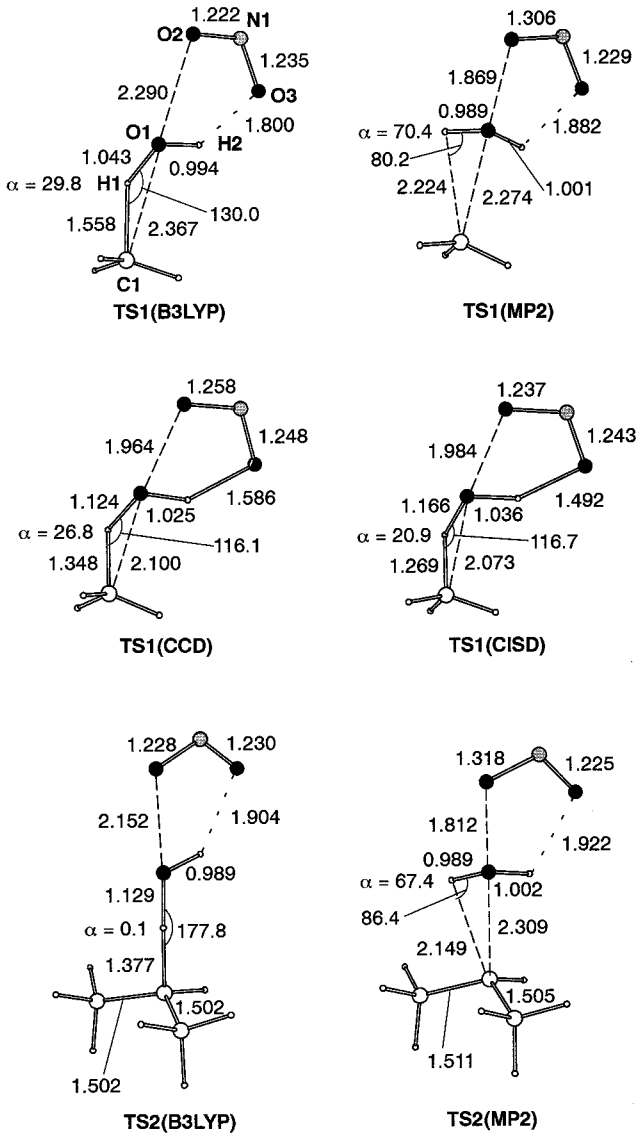

Figure 1. B3LYP, MP2, CCD, and CISD structures of the concerted transition state for the oxidation of methane and propane with peroxynitrous acid calculated with the 6-31+G* basis set.

and 67.4°, respectively, of the new O1−H1 bond with respect to the O2−O1−H2 plane (Figure 1).

Unlike **TS1(MP2)** and **TS2(MP2)**, the B3LYP transition structures,[32] **TS1(B3LYP)** and **TS2(B3LYP)**, calculated with the 6-31+G* basis set (Figure 1) have a net positive charge on the R_2CH moiety (+0.124e and +0.144e, respectively). Hence the B3LYP transition states have a *hydride transfer character*. The geometry of these transition states is determined mainly by involvement of the σ^*_{OO} orbital of ONOOH. This is indicated by a greater O−O distance and a much smaller out-of-plane α angle (Figure 1, Table S5). The more linear arrangement of the O1- -H1- -C1 atoms and the increase in the net positive charge on the Me_2CH fragment in **TS2(B3LYP)** compared to **TS1-(B3LYP)** indicate progressive development of hydride transfer character with an increase in the number of the methyl groups at the reaction carbon center. The role of the HOMO (π^*_{OO}) has diminished almost to zero. Thus the B3LYP/6-31+G* calculations predict electrophilic insertion of the terminal oxygen atom of peroxynitrous acid into a CH bond of methane and propane. Optimization using the more flexible 6-311+G** and 6-311++G(3df,2pd) basis sets produced little change in the geometry of **TS1(B3LYP)** (Table S5).

Geometries of the transition state for the oxidation of methane with ONOOH optimized at the CISD/6-31+G* and CCD/6-31+G* levels also correspond to the electrophilic oxygen insertion into the CH bond. The CISD and CCD structures of **TS1** are characterized by even smaller out-of-plane α angles than the B3LYP one (Figure 1) and values of the O1−H1−C1 bond angle in these structures are closer to that in **TS1(B3LYP)** than in **TS1(MP2)**, although the CISD and CCD calculations predict a greater synchronicity in the formation of the new O1−H1 bond and cleavage of the old C1−H1 bond. Thus, as in the case of the dioxirane oxidation of alkanes,[30] the B3LYP method describes the nature of the transition states of the oxidation of aliphatic CH bonds with ONOOH more adequately than does the MP2 method.

All B3LYP calculations with the 6-31+G*, 6-311+G**, and 6-311++G(3df,2pd) basis sets as well as the QCISD(T)/6-31+G*//B3LYP/6-31+G* calculations give similar values of activation energy, 31 ± 3 kcal mol^{-1}, for the oxidation of methane with ONOOH (Table 1). Rather higher barriers of 42 ± 2 kcal mol^{-1} are obtained at the MP2, QCISD(T)//MP2, QCISD(T)//CISD, and CCSD(T)//CCD levels using the 6-31+G* basis set. A similar ratio between B3LYP activation barriers and the barriers derived with the MP2, QCISD(T)//MP2, and QCISD(T)//CISD calculations was observed earlier[21] for epoxidation and heteroatom oxidation reactions of peroxynitrous acid. Bach et al.[21] recommended the QCISD(T) level of theory applied to B3LYP structures as the most economical and accurate protocol for the calculations of activation barriers for the peroxynitrite oxidations. We used this protocol for calculations of the oxidations of isobutane, propene, and 1,4-pentadiene.

Like **TS2(B3LYP)**, transition state **TS3**[32] of the oxidation of the tertiary CH bond in isobutane with ONOOH has the linear configuration of the C1- -H1- -O1 fragment (Figure 2). Transition state **TS3** is more early in comparison with **TS2(B3LYP)** because **TS3** is characterized by shorter C1−H1 and O1−O2 distances and by a longer O1−H1 distance. Correspondingly, **TS3** has a smaller relative energy (Table 3) and a smaller charge transfer from the hydrocarbon moiety to the NO_2 group: according to the NBO-B3LYP/6-31+G* calculations, net charges on the alkyl and NO_2 groups in **TS3** are 0.085e and −0.217e, relatively, versus 0.144e and −0.239e in **TS2-(B3LYP)**.

Investigation of the IRC potential energy profiles calculated by B3LYP/6-31+G* for the oxidations of methane and propane with ONOOH reveals that the transition structures **TS1(B3LYP)** and **TS2(B3LYP)** correspond to a concerted mechanism. The electrophilic oxygen insertion proceeds from the hydrocarbon and peroxynitrous acid reactants to the corresponding alcohol and nitrous acid, HNO_2, products with no intervening minima. By contrast, the IRC-B3LYP/6-31+G* calculations for the oxidation of isobutane via **TS3** in the product direction "crashed" after attaining structure **B3**[33] (Figure 2). The natural population analysis of this structure revealed a considerable charge separation between the $(CH_3)_3C$ (0.499e) and NO_2 (−0.456e) groups.

(32) RB3LYP wave functions for all B3LYP/6-31+G* transition states **TS1**−**TS5** of the CH oxidations with ONOOH suffer from a RHF → UHF instability. Geometry reoptimizations of the singlet **TS1**−**TS5** at the UB3LYP/6-31+G* level produced structures identical in geometry and energy to those obtained by RB3LYP.

(33) The structure **B3** and the similar structures **B4** and **B5** (Figures 2 and 3) were the last optimized structures of the IRC-B3LYP/6-31+G* paths toward the products. Attempts at convergence of the next points of the potential energy surfaces could not be achieved even after 100 optimization steps. Such "crashes" may be an indication of the presence of a bifurcation point in the reaction coordinate.

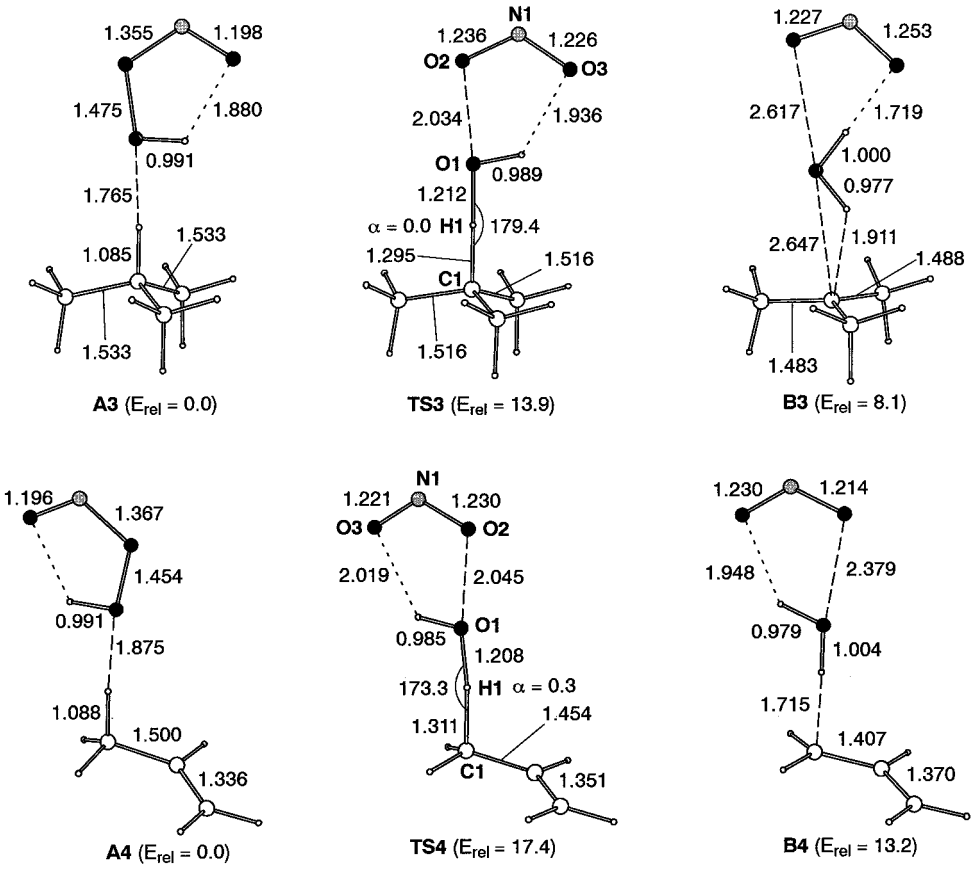

Figure 2. B3LYP/6-31+G* structures of the transition states for the oxidation of isobutane and propene with peroxynitrous acid along with structures **A3**, **A4**, **B3**, and **B4** derived with the IRC-B3LYP/6-31+G* calculations. The IRC relative energies (in kcal mol^{-1}) are not ZPVE corrected.

Geometry optimization starting from **B3** at the B3LYP/6-31+G* level yielded a complex of *tert*-butyl alcohol and nitrous acid with an energy of −58.4 kcal mol^{-1} (including Δ*Z*PVE) with respect to the initial reactants. The reaction path toward the reactants produces structure **A3**,[34] from the geometry of which (Figure 2) one can see that ONOOH attacks isobutane precisely along the tertiary CH bond.

(ii) Path b. The free radical path toward $R_2(R')C^{\bullet}$, water, and $ONO^{\bullet}$ is much less favorable thermodynamically than the formation of methanol, 2-propanol, and *tert*-butyl alcohol in the reactions of methane, propane, and isobutane with ONOOH through path a. All methods used in the present study indicate a high exothermicity for the direct hydroxylation (−43, −53, and −55 kcal mol^{-1} for methane, propane, and isobutane). On the other hand, formation of the free radical products is endothermic for the oxidation of methane, practically thermoneutral for propane, and only slightly exothermic for isobutane (Tables 1−3).

(iii) Path c. As it was discussed in the Introduction, besides the direct induction of the free radical oxidation by peroxynitrous acid itself, there is the other free radical pathway (Scheme 1, path c) which involves the initial homolysis of the O−O bond in ONOOH. The enthalpy of homolysis of peroxynitrous acid, calculated at the same levels of theory as the oxidation of methane, propane, and isobutane (ca. 14 kcal mol^{-1}), is underestimated by about 8 kcal mol^{-1}, compared to our G2(MP2-B3LYP) value (21.5 kcal mol^{-1}) and experiment (Table 4). Nevertheless, this value is substantially smaller than the activation enthalpies of the two-electron oxidation of these alkanes (Tables 1−3). Moreover, the entropy factor ($T\Delta S$) has to work in favor of the homolysis. For example, in the case of the concerted oxidation of propane (Scheme 1, path a), the QCISD(T)/6-31+G*//B3LYP/6-31+G* values of the activation enthalpy ($\Delta H^{\neq}_{298}$) and entropy ($\Delta S^{\neq}_{298}$) are 18.3 kcal mol^{-1} and −21.6 cal mol^{-1} K^{-1}, respectively, corresponding to a free energy of activation, $\Delta G^{\neq}_{298}$ = 24.7 kcal mol^{-1}. This value is considerably greater than the free energy of the gas-phase homolysis of ONOOH, 12.2 kcal mol^{-1}, from ΔS_{298} = 36.0 cal mol^{-1} K^{-1} calculated at the same level and ΔH_{298} = 22.9 kcal mol^{-1} calculated at the G2(MP2-B3LYP) level. Other theoretical (9.3 kcal mol^{-1})[11] and experimental estimates (13.8 and 17.4 kcal mol^{-1})[8,13] of the energy of homolysis are also smaller than the obtained free energy of activation for the "path a" oxidation of propane with ONOOH.

These results are not consistent with the conclusions of Rudakov and co-workers.[19] However, the complex kinetic scheme of these workers appears not to have taken into account O_2 production during the decomposition of ONOOH and the rapid reaction of hydroxyl radicals with peroxynitrite anion.[13] Moreover, the kinetic curves of accumulation of cyclohexanol and cyclohexanone for the peroxynitrite oxidation of cyclohexane given in the work[19] indicate a simultaneous rather than consecutive formation of these products. The product distribution can be explained by the formation of cyclohexylperoxyl radical, decomposition of which leads to the simultaneous formation of the ketone and alcohol (Scheme 5). Such a mechanism of the decomposition of alkylperoxyl radicals into the corresponding ketones and alcohols was earlier proposed by von Sonntag

(34) Structures **A3**, **A4**, and **A5** are only intermediate points belonging to the corresponding IRC-B3LYP/6-31+G* curves. True local minima corresponding to complexes of the reactants can be attained by continuation of the IRC-3LYP/6-31+G* calculations.

Scheme 5

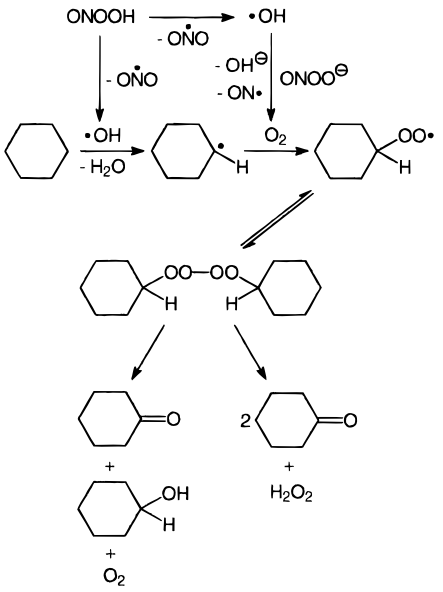

and co-workers.[35] The ratio of cyclohexanone/cyclohexanol (2:1) found for the peroxynitrite oxidation of cyclohexane[19] is in agreement with Scheme 5 and is quite similar to the ratio of 2.7:1 obtained[35] for the γ-radiolysis of cyclohexane in N_2O/O_2 saturated aqueous solutions. In both cases, the cyclohexylperoxyl radical is formed in the reaction of O_2 with cyclohexyl radical and the latter is the product of the hydrogen abstraction from cyclohexane by the hydroxyl radical.

Peroxynitrous Acid. Oxidation of Allylic CH Bonds in the Unsaturated Hydrocarbons: (i) Path a. The B3LYP/6-31+G* optimized structures[32] of transition states **TS4** and **TS5** of the oxidation of propene and 1,4-pentadiene with ONOOH are similar in their geometry to the transition state **TS3** of the oxidation of isobutane (Figures 2 and3). These structures are characterized by an almost linear arrangement of the C1- -H1- -O1 atoms. The ratio of the C1−H1, O1−O2, and O1−H1 distances indicates that **TS4** is rather later than **TS3**, and **TS5** is earlier.

There is a smaller charge transfer to the NO_2 group in **TS4** (net charge on the NO_2 group is −0.158e) and **TS5** (−0.134e) in comparison with **TS1** (−0.256e), **TS2** (−0.238e), and **TS3** (−0.217e). The positive net charge (0.047e) on the alkyl group in **TS4** is also smaller than in **TS1** (0.124e), **TS2** (0.144e), and **TS3** (0.085e). The hydrocarbon moiety in **TS5** even bears a slightly negative net charge (−0.017e), although on the basis of the geometry of the transition state, one can exclude any involvement of the HOMO (π_{OO}*) of peroxynitrous acid in a proton abstraction-like process. The depolarization of transition states **TS4** and **TS5** is probably a consequence of their shift toward the initial reactants on the potential energy surfaces and/or of the greater diradical character of these species. However, the natural population analysis of structures[33] **B4** and **B5** (Figure 2 and 3), lying on the IRC-B3LYP/6-31+G* curves from **TS4** and **TS5** toward the products, indicated a substantial development of a carbocationic character of the alkyl group and an anionic character of the nitrite group. For example, the structure **B5** can be described as an ionic pair of the pentadienyl cation (positive net charge is 0.512e) and the nitrite anion (−0.547e) separated by a water molecule. The structure **B4** that is closer to **TS4** on the reaction coordinate has a smaller charge separation: 0.218e on the allyl group and −0.224e on the nitrite group. As in the case of **B3**, a full B3LYP/6-31+G* optimization starting from the structures **B4** and **B5** gave complexes of nitrous acid and the corresponding alcohols with relative energies of −51.0 and −55.4 kcal mol^{-1} (including ΔZPVE).

(ii) Path b. The allylic CH bonds in propene (BDE = 88.6 kcal mol^{-1})[36] and 1,4-pentadiene (79.9 kcal mol^{-1})[37] are substantially weaker than the secondary CH bonds in propane (98.6 kcal mol^{-1})[38] or the tertiary CH bond in isobutane (96.5 kcal mol^{-1}).[38] Indeed, the formation of a radical pair, CH_2=CH(R)CH$^•$ and ONO$^•$, and H_2O in the reactions of propene and 1,4-pentadiene with ONOOH was found to be much more exothermic, −10 and −20.5 kcal mol^{-1}, relatively, than in the case of propane and isobutane, −0.3 and −2.1 kcal mol^{-1}, at the QCISD(T)/6-31+G*//B3LYP/6-31+G* level.[39] However, the concerted pathway toward the corresponding alcohols, i.e., allyl alcohol (−46.9 kcal mol^{-1}) and penta-1,4-dien-3-ol (−49.6 kcal mol^{-1}), remains thermodynamically favorable. Therefore, direct induction of the free radical mechanism by peroxynitrous acid in its reaction with lipids is unlikely.

(iii) Path c. According to the experimental works,[17,18] the reaction of peroxynitrous acid with lipids probably does follow a free radical pathway. In this case, the reactive species is simply the discrete hydroxyl radical generated in homolysis of the O−O bond in ONOOH. It is important that both theoretical[11] [12.2 (this work) and 9.3 kcal mol^{-1}] and experimental[8,13a] (13.8 and 17.4 kcal mol^{-1}) estimates of free energy for the homolysis are lower than the lower limit for the free energy of activation for the direct hydroxylation of 1,4-pentadiene (model for lipids), $\Delta G^{\neq}_{298}$ = 20.5 kcal mol^{-1} ($\Delta H^{\neq}_{298}$ = 13.5 kcal mol^{-1}, $\Delta S^{\neq}_{298}$ = −23.6 cal mol^{-1} K^{-1}), obtained on the basis of the B3LYP/6-31+G* relative energy of **TS5** (Table 6). This is in agreement with experiment,[18a] according to which lipid hydroperoxides (LOOH) are major products and alcohols (LOH) are minor ones of the reaction of lipids (L) with ONOOH in the presence of O_2.

Epoxidation of C=C Bonds in Lipids: An Alternative Path? There is also another competitive reaction, the epoxidation of C=C bonds in unsaturated hydrocarbons with peroxynitrous acid. The B3LYP/6-31+G* calculations gave practically identical potential barriers[40] for the epoxidations of 1,4-pentadiene and propene: 11.1 and 10.7 kcal mol^{-1}, respectively. A more accurate QCISD(T)/6-31+G*//B3LYP/6-31+G* value of the activation energy for the epoxidation of propene, 11.8 kcal mol^{-1}, is quite close to the B3LYP value, but somewhat smaller than the value of 15.5 kcal mol^{-1} calculated by Bach et al.[21] at the QCISD(T)/6-31G*//QCISD/6-31G* level.

Although the B3LYP/6-31+G* activation enthalpy for the epoxidation of 1,4-pentadiene with peroxynitrous acid is rather

(35) Zegota, H.; Schuchmann, M. N.; von Sonntag, C. *J. Phys. Chem.* **1984**, *88*, 5589.

(36) Ochterski, J. W.; Petersson, G. A.; Wiberg, K. B. *J. Am. Chem. Soc*. **1995**, *117*, 11299.

(37) Ruscic, B.; Berkowitz, J. *J. Chem. Phys*. **1992**, *92*, 1818.

(38) Berkowitz, J.; Ellison, G. B.; Gutman, D. *J. Phys. Chem*. **1994**, *98*, 2744.

(39) The QCISD(T)/6-31+G*//B3LYP/6-31+G* calculations satisfactorily reproduce thermochemistry of unsaturated hydrocarbons and their radicals. Indeed the bond dissociation enthalpy (BDE), ΔH_{298}, calculated for propene from an isodesmic reaction CH_2=CH−CH_3 + $CH_3CH_2^•$ → CH_2=CH−$CH_2^•$ + CH_3CH_3, is 88.3 kcal mol^{-1} and for 1,4-pentadiene, calculated from an isodesmic reaction $(CH_2$=$CH)_2CH_2$ + $(CH3)_2CH^•$ → $(CH_2$=$CH)_2CH^•$ + $(CH_3)_2CH_2$, is 77.8 kcal mol^{-1}. The corresponding experimental values are 88.6 kcal mol^{-1} for propene[36] and 79.9 kcal mol^{-1} for 1,4-pentadiene.[37] Experimental BDEs[38] of 101.1 kcal mol^{-1} for ethane and 98.6 kcal mol^{-1} for propane were used in these calculations.

(40) B3LYP/6-31+G* structures of the transition states for the epoxidation of propene and 1,4-pentadiene with ONOOH and $ONOO^-$ along with their relative energies are given in Figures 1S and 2S of the Supporting Information.

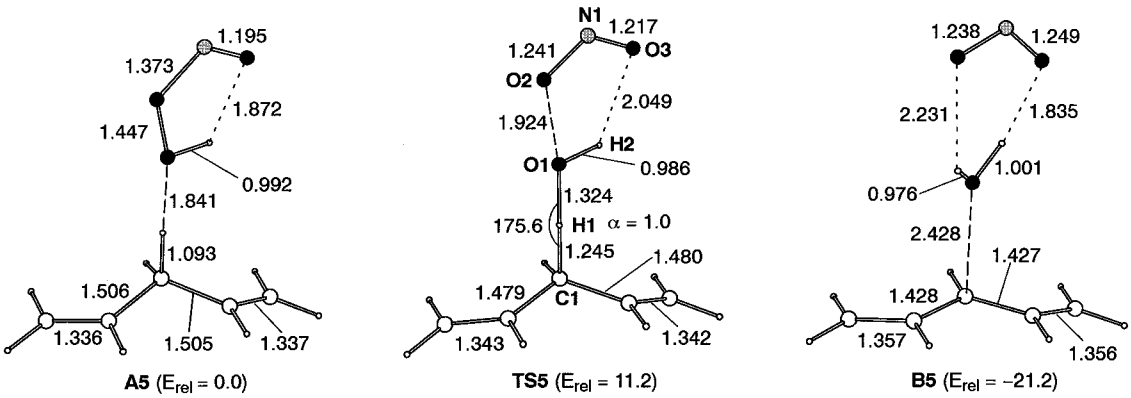

Figure 3. B3LYP/6-31+G* structures of the transition state for the oxidation of 1,4-pentadiene with peroxynitrous acid along with structures **A5** and **B5** derived with the IRC-B3LYP/6-31+G* calculations. The IRC relative energies are not ZPVE corrected.

lower than the enthalpy of homolysis of the O−O bond in this acid (Table 4), the entropy factor, $T\Delta S$, works again in favor of the homolysis. Both our B3LYP/6-31+G* value of free energy of activation for the epoxidation, $\Delta G^{\neq}_{298} = 18.9$ kcal mol^{-1} ($\Delta H^{\neq}_{298} = 11.2$ kcal mol^{-1}, $\Delta S^{\neq}_{298} = -25.9$ cal mol^{-1} K^{-1}), and ca. 23 kcal mol^{-1} using the data of Bach et al.[21] are higher than the estimated values of free energy for the O−O homolysis (vide supra). Thus the epoxidation and direct hydroxylation can be considered as minor side processes in the oxidative damage of lipid membranes by peroxynitrous acid. The major pathway involves the generation of free radicals, L$^{\bullet}$, which subsequently react with O_2 to give hydroperoxides, LOOH (Scheme 2).

Peroxynitrite Anion. Oxidation of CH Bonds in Saturated and Unsaturated Hydrocarbons. Unlike the CH oxidations with peroxynitrous acid, there are no significant differences in the structures and the nature of the transition states for the oxidations with peroxynitrite anion, i.e., they were independent of the method of the calculation. All methods (B3LYP, MP2, CCD, and CISD) employed here give nearly identical structures for transition state **TS1A** for the oxidation of methane with $ONOO^-$ (Figure 4). Similar structures were obtained by the B3LYP and MP2 calculations for transition state **TS2A** for propane. The geometrical parameters and energies of the B3LYP/6-31+G* structures **TS1A**, **TS2A**, and **TS4A** are the same either with the C_s symmetry or without geometry constraints in the optimization.

Like **TS1**−**TS5**, transition states **TS1A**−**TS5A**[41] indicate asynchronous bond breaking and bond making, i.e., they are characterized by a nearly completely formed new bond O1−H1 and the already broken bonds O1−O2 and C1−H1 (Figure 4, Table S1). Together with the antibonding σ^*_{OO} orbital (LUMO+1), the HOMO-1 of peroxynitrite anion is substantially involved in formation of **TS1A**−**TS5A**. The HOMO-1 is mainly the nonbonding orbital of the O1 atom of the anion, lying in the molecular plane of the anion (Chart 1). The geometric consequence of the involvement of this orbital is bending of the C1- -H1- -O1 fragment in the plane of the leaving O2N1O3 group. This is also supported by NBO population analysis, which indicates a net negative charge on the hydrocarbon moiety in all B3LYP/6-31+G* transition states **TS1A** (−0.238e), **TS2A** (−0.165e), **TS3A** (−0.184e), **TS4A** (−0.465e), and **TS5A** (−0.741e).

IRC-B3LYP/6-31+G* potential energy curves for the CH oxidation of either saturated (methane, propane,and isobutane) or unsaturated hydrocarbons (propene and 1,4-pentadiene) with peroxynitrite anion predict a smooth progression toward the corresponding alcohols and NO_2^-. Estimation of the thermo-

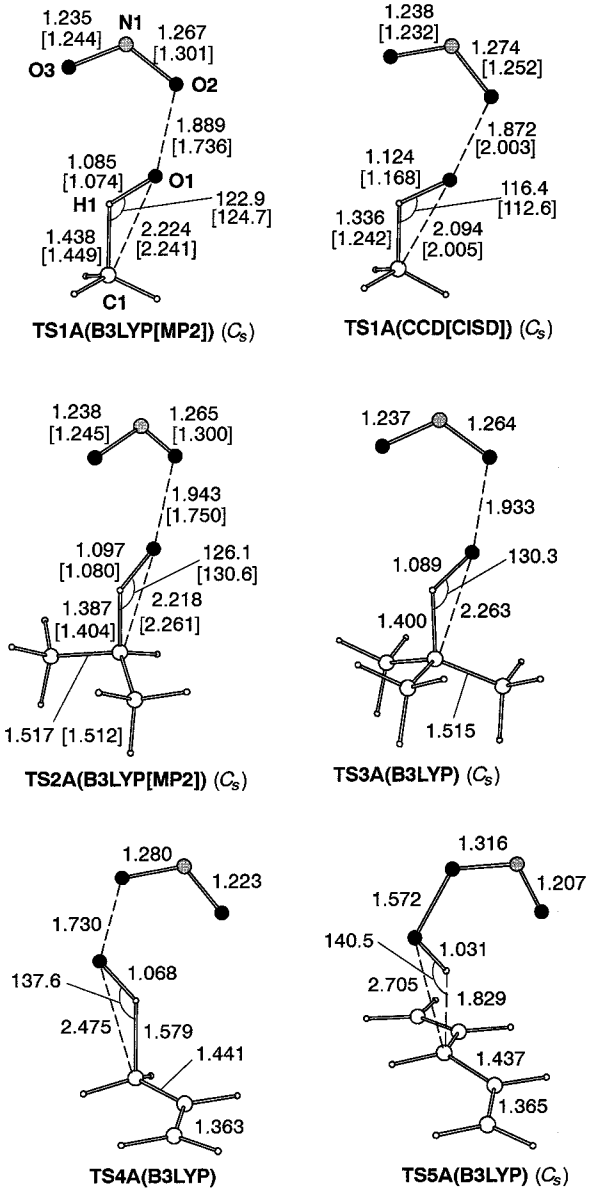

Figure 4. B3LYP, MP2, CCD, and CISD structures of the concerted transition state for the oxidation of methane, propane, isobutane, propene, and 1,4-pentadiene with the peroxynitrite anion calculated with the 6-31+G* basis set.

(41) The RB3LYP solutions for these transition structures were found to be both singlet and triplet stable, while the RHF solutions for the MP2 structures of **TS1A** and **TS2A** exhibit a RHF → UHF instability.

chemical balances of the possible pathways for the oxidations excludes the possibility of a free radical mechanism analogous to the neutral peroxynitrous acid oxidation in the gas phase. Even for the most stable 1,4-pentadienyl radical, the reaction heats for the formation of either $(CH_2{=}CH)_2CH^{\bullet} + ONO^{\bullet} + OH^-$ or $(CH_2{=}CH)_2CH^{\bullet} + OH^{\bullet} + ONO^-$ are highly positive (Table 6). On the other hand the concerted path of the direct hydroxylation is highly exothermic in all cases (Tables 1, 2, 3, 4, and 6).

Thus all transition states of CH oxidation with $ONOO^-$ studied here have the same nature: electrophilic oxygen insertion into the aliphatic CH bond, together with a substantial polarization in the sense of *proton transfer* from the substrate to the oxidant.

As one can see from the case of the parent system, methane−$ONOO^-$, all structures of **TS1A** optimized with different methods have similar geometrical parameters and similar single point QCISD(T) relative energies, ca. 36 kcal mol^{-1} (Table 1). The B3LYP calculations using the extended basis sets of 6-311+G** and 6-311++G(3df,2pd) give rather lower activation barriers for the oxidation of methane with peroxynitrite anion.

For the competitive reaction of epoxidation[40] of propene with $ONOO^-$, both the B3LYP/6-31+G* and QCISD(T)/6-31+G*//B3LYP/6-31+G* methods predict a smaller activation enthalpy of 15.2 and 12.5 kcal mol^{-1}, respectively, than for the oxidation of an allylic CH bond, 20.2 and 25.0 kcal mol^{-1}. In the case of 1,4-pentadiene, the B3LYP/6-31+G* potential barrier for the epoxidation,[40] 12.7 kcal mol^{-1}, is higher than the barrier of the CH oxidation (Table 6) by 4.3 kcal mol^{-1}.

According to the B3LYP/6-31+G* and QCISD(T)/6-31+G*//B3LYP/6-31+G* calculations, the oxidative reactivity of the "naked" peroxynitrite anion is lower than the reactivity of peroxynitrous acid only in the reactions with propane and isobutane. With respect to the other three hydrocarbons, the reactivities of these oxidants are comparable (Tables 1, 2, 3, 4, and 6). The QCISD(T)/6-31+G*//B3LYP/6-31+G* activation barrier for the CH oxidation of 1,4-pentadiene with the "naked" peroxynitrite anion in the gas phase is somewhat lower than the barrier for the oxidation with ONOOH. The value of this barrier, 14 kcal mol^{-1}, suggests that the nonsolvated peroxynitrite anion, if transferred into an intramembrane medium by a lipophilic counterion, can be a powerful two-electron oxidant of allylic CH bonds in lipids.

Effects of Aqueous Medium. In water at pH <10, peroxynitrite anion is in equilibrium with its conjugate acid, in which homolysis of the O−O bond can occur to give a more reactive oxidative species. Under such conditions, the two-electron oxidation by peroxynitrite anion cannot compete with either the oxidation by peroxynitrous acid or the homolysis of this acid. Even an approximate SCIPCM modeling of the aqueous medium ($\epsilon = 78.54$) with SCRF-B3LYP/6-31+G* calculations predicts a considerable increase of all of the activation barriers for CH oxidations with $ONOO^-$ while the barriers for the oxidations with ONOOH and for its homolysis are decreased (Tables 2−6). In the modeled water medium, the differences of the B3LYP/6-31+G* potential barriers, $E_a^{anion} - E_a^{acid}$, for the reactions with propane, propene, and 1,4-pentadiene are 20.0, 18.6, and 15.6 kcal mol^{-1}, respectively. In the gas phase, these differences are 68.9, 2.3, and −4.8 kcal mol^{-1}. A similar picture is observed for the epoxidations[40] of propene and 1,4-pentadiene by ONOOH and its anion. The B3LYP/6-31+G* differences $E_a^{anion} - E_a^{acid}$, 4.5 and 1.6 kcal mol^{-1}, respectively, calculated at the gas-phase approximation increase to 18.2 and 16.5 kcal mol^{-1} in the aqueous medium. Finally, in the gas phase, the B3LYP/6-31+G* activation enthalpy for the CH oxidation with peroxynitrite anion is lower by 5.7 kcal mol^{-1} than the energy of the homolysis of peroxynitrous acid. In water, the activation enthalpy for the oxidation becomes higher than the energy of the homolysis by 15.3 kcal mol^{-1}. In general, this is in accord with the main body of experimental data[1−3] on low rates of peroxynitrite oxidations of organic substrates in water at pH <10 in the absence of a "promoter" such as carbon dioxide.

Conclusions

The principal pathway for the oxidation of saturated and unsaturated hydrocarbons by peroxynitrous acid is via hydroxyl radicals produced upon homolysis of the O−O bond. The direct two-electron oxidation of aliphatic CH bonds in saturated and unsaturated hydrocarbons is a highly exothermic process which leads to the corresponding alcohols having a higher free energy of activation in all of the cases studied. The transition state of the electrophilic oxygen insertion has mainly hydride transfer character. The energetic, structural, and electronic aspects of the oxidation of CH bonds in methane, propane, and isobutane with peroxynitrous acid are very similar to those of the oxidations with dioxiranes. The free radical pathway (single-electron oxidation) induced by peroxynitrous acid itself is thermodynamically less favorable than the concerted pathway (two-electron oxidation) even in the case of the oxidation of an allylic CH bond in 1,4-pentadiene, and has the same high free energy of activation.

Therefore, the present theoretical study supports a hypothesis that the reactive species in the lipid peroxidation with peroxynitrous acid in the presence of O_2 is the discrete hydroxyl radical, which is formed in homolysis of the O−O bond in this acid. The direct hydroxylation of allylic CH bonds and the epoxidation of C=C bonds are predicted to have higher activation energies in comparison with the energy of homolysis and must occur as minor side reactions. This is in agreement with observations[17,18] of lipid peroxidation induced by peroxynitrous acid.

The more stable nonsolvated ("naked") peroxynitrite anion, if transferred into the intramembrane medium by a lipophilic counterion, is predicted to be a powerful oxidant of allylic CH bonds in lipids. This anion oxidizes CH bonds in saturated and unsaturated hydrocarbons via a concerted mechanism of the electrophilic oxygen insertion abetted by nucleophilic proton abstraction. Thus the transition state of the direct hydroxylation by the anion has mainly proton-transfer character due to involvement of the nonbonding orbital of the terminal oxygen atom.

Acknowledgment. The financial support of the Natural Sciences and Engineering Research Council of Canada is gratefully acknowledged. We thank Professors David Armstrong and Clemens von Sonntag for helpful comments during the drafting of this paper.

Supporting Information Available: Tables S-1, S-2, S-3, and S-4 listing total energies and zero-point corrections of all studied species, and Table S-5, which gives geometrical details for the transitions structures of methane oxidation by ONOOH and $ONOO^-$ and Figures 1S and 2S showing B3LYP/6-31+G* structures of the transition states for the epoxidation of propene and 1,4-pentadiene with ONOOH and $ONOO^-$ along with their relative energies (PDF). This material is available free of charge via the Internet at http://pubs.acs.org.

JA993533K